

Laughlin state on stretched and squeezed cylinders and edge excitations in the quantum Hall effect

E. H. Rezayi

Department of Physics and Astronomy, California State University at Los Angeles, Los Angeles, California 90032

F. D. M. Haldane

Department of Physics, Princeton University, Princeton, New Jersey 08544

(Received 21 June 1994)

We study the Laughlin wave function on the cylinder. We find it only describes an incompressible fluid when the two lengths of the cylinder are comparable. As the radius is made smaller at fixed area, we observe a continuous transition to the charge-density-wave Tao-Thouless state. We also present some exact properties of the wave function in its polynomial form. We then study the edge excitations of the quantum Hall incompressible fluid modeled by the Laughlin wave function. The exponent describing the fluctuation of the edge predicted by recent theories is shown to be identical with numerical calculations. In particular, we obtain the occupation amplitudes of edge state $n(k)$ for four to ten electron-size systems. When plotted as a function of the scaled wave vector they become essentially free of finite-size effects. The resulting curve obtains a very good agreement with the appropriate infinite-size Calogero-Sutherland model occupation numbers. Finally, we numerically obtain $n(k)$ of the edge excitations for some pairing states which may be relevant to the $\nu = \frac{5}{2}$ incompressible Hall state.

It is now well-established that the quantum Hall effect (QHE) in the spin-polarized two-dimensional (2D) electron liquid at Landau-level filling factor $\nu = 1/q$ results from an incompressible correlated electron state which is very well described by the simple model wave functions introduced by Laughlin.¹ This has been verified by extensive numerical studies² of systems of a finite number N of electrons which have been carried out in two popular geometries: spherical³ and periodic, or toroidal.^{4,5}

These geometries are convenient for obtaining bulk properties by extrapolation to the thermodynamic limit as they do not introduce edges. In the most symmetric spherical geometry, the geometry is fully specified by the requirements of translational and rotational symmetry; in the periodic case, rotational symmetry is absent, and while the *area* of the elementary cell is fixed by the integrally quantized number of magnetic-flux quanta that pass through the surface, the Bravais lattice of translations in which physical (gauge-invariant) quantities are formulated can be continuously varied. When the shortest of these translations has a length comparable to or shorter than a magnetic length (or than the mean bulk interparticle spacing) one may expect that the results of the finite-size calculation are no longer representative of the bulk physics.

There are other geometries in which the QHE has been discussed; in particular, *cylindrical* geometry appears well suited for studies of *edge states* associated with the boundaries of a region of incompressible fluid. In this geometry, there are two characteristic lengths in the N -electron system: one is the periodic repeat distance (circumference of the "cylinder") which plays the role of the shortest translation in the periodic system; the other is the width of the finite strip of incompressible fluid that

results when the electrons are confined in the well of a potential that varies in the direction parallel to the axis of the cylinder. When this length becomes small, there are interactions between the two edges of the fluid, and calculations in this limit (unlike the case of small periodic repeat distance) are presumably relevant to the physics of the QHE in narrow channels.

In this paper, we describe the properties of the Laughlin wave function on the cylinder as the circumference of the cylinder is varied at fixed particle number (i.e., fixed surface area of the incompressible fluid) and study its' edge excitations. As usual, we only consider electrons restricted to states within the lowest Landau level.

The Laughlin wave function on the cylinder⁶ for $\nu = 1/m$ is given by

$$\Psi_L = \prod_{i < j} (e^{i\gamma z_i/l} - e^{i\gamma z_j/l})^m \prod_i e^{-y_i^2/2l^2}, \quad (1)$$

where $\gamma = l/R$, $l = (\hbar/eB)^{1/2}$ is the magnetic length, and R is the radius of the cylinder. The complex coordinate z is $x + iy$, where x is the periodic coordinate along the circumference of the cylinder and y is along the axis.

The periodicity in the x direction means that the allowed pseudomomentum k_x of each particle is quantized: $k_x = n/R$, where the integer n labels the conventional basis of single-particle "Landau-gauge" states. We allow the range of y to become infinite, but "compress" the electrons by restricting them to the Landau-gauge states with n in the range $0, 1, 2, \dots, N_\phi$. Just as in the spherical geometry, the Landau-level degeneracy is equal to $N_L = N_\phi + 1$, which is proportional to the area available for the guiding center motion.

It is important to note that the study of many-particle

states on the cylinder is different from other geometries because of a similar degeneracy if the ground state is an incompressible fluid. In this case, the fluid will determine its own density and need not occupy the entire surface available to it, but will form a “ribbon” on the cylinder. The displacement of this ribbon as a whole will cause an overall degeneracy. For finite systems, interactions with the edges will lift these into quasidegeneracies. As a result, care needs to be exercised in sorting out the internal excitations from the translational modes.

We construct the Laughlin wave function Ψ_L numerically as the only zero energy state of the hard-core potential with pseudopotential parameters $V_m \neq 0$ for $m = 0, 1, \dots, \nu^{-1} - 1$, where V_m are the pair energies in the state of relative angular momentum m .

The Hamiltonian can be obtained by a generalization of the pseudopotential formulation² to the cylinder as follows:

$$H = \frac{\gamma}{2\pi} \sum_{i < j, n, m} \int_{-\infty}^{\infty} dq V_m L_m (q^2 l^2 + \gamma^2 n^2) e^{-q^2 l^2 / 2} \times e^{-\gamma^2 n^2 / 2} e^{i\gamma n \hat{y}_i / l} \times e^{iq(\hat{x}_i - \hat{x}_j)} e^{-i\gamma n \hat{y}_j / l}. \quad (2)$$

The parameter γ serves as an “aspect ratio” (we fix the area to preserve the Landau-level degeneracy), and it proves to be the crucial parameter in determining whether the ground state is an incompressible fluid or not. For finite systems, the physical properties of Ψ_L depend strongly on γ . For $\gamma \geq 0.7$, Ψ_L becomes different from an incompressible uniform fluid and begins to approach a charge-density-wavelike state, which for larger γ (≈ 1.2)

is essentially described by the Tao-Thouless⁷ (TT) state.

To investigate the γ dependence, we note that in occupation space Ψ_L has the general form,

$$\Psi_L = \sum_{\{n_i\}} A(n_1, n_2, \dots, n_N) \prod_i (e^{i\gamma z_i})^{n_i} \prod_i e^{-y_i^2 / 2l^2} \quad (3)$$

$$= \sum_{\{n_i\}} \frac{A(n_1, n_2, \dots, n_N)}{\{a(\gamma)\}^N} \prod_i (e^{\gamma^2 n_i^2 / 2}) \prod_i \Psi_{n_i}(z_i). \quad (4)$$

$A(n_1, n_2, \dots, n_N)$ are amplitudes *independent* of γ , $a(\gamma)$ is an overall normalization factor *independent* of the occupation numbers, and $\Psi_n(z)$ are the appropriate single-particle wave functions. An algorithm for calculating these amplitudes for small system sizes has been given previously,⁸ but this does not appear to provide any substantial advantage to the alternative of diagonalizing H directly. Accordingly, we calculate Ψ_L numerically from H for $\gamma = 0$ and then construct it for $\gamma \neq 0$ from Eq. (4). The charge densities shown in Figs. 1 and 2 were obtained in this manner. The parameter a in the figures is the aspect ratio: $a = L / (2\pi R) = (\gamma^2 \times N_L) / 2\pi$, where L is the length of the cylinder. The square points in Figs. 1 and 2 are the average occupation of each orbital positioned at the center of the Gaussian envelope of the orbital, which are separated by $\Delta y = \gamma$. These figures capture the transition to the charge density wave state as γ is increased.

The extremely squeezed cylinder (hoop geometry) is realized at $\gamma = 0$; this is an interesting limit where the spatial dimensions have been reduced to essentially 1 in that the Gaussian envelopes are always centered at $y = 0$. The density, however, does have a finite width in the

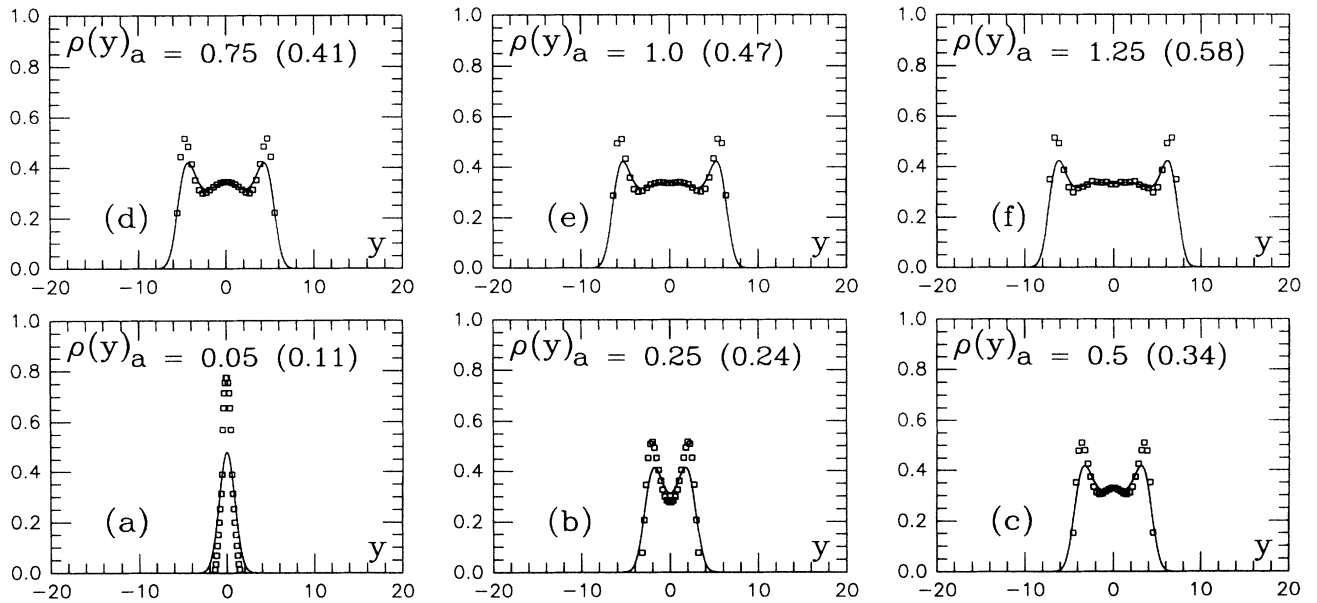


FIG. 1. The charge density plotted versus y , the dimension along the length of the cylinder, for $N = 10$. Also plotted are the average occupations of the Landau-level orbital placed at the position of the guiding centers. The aspect ratios $a = L / 2\pi R$ are also indicated on each plot; γ is given in parentheses. The series of plots shows the evolution of the incompressible fluid from the squeezed cylinder in the lower left corner as γ is increased to the right.

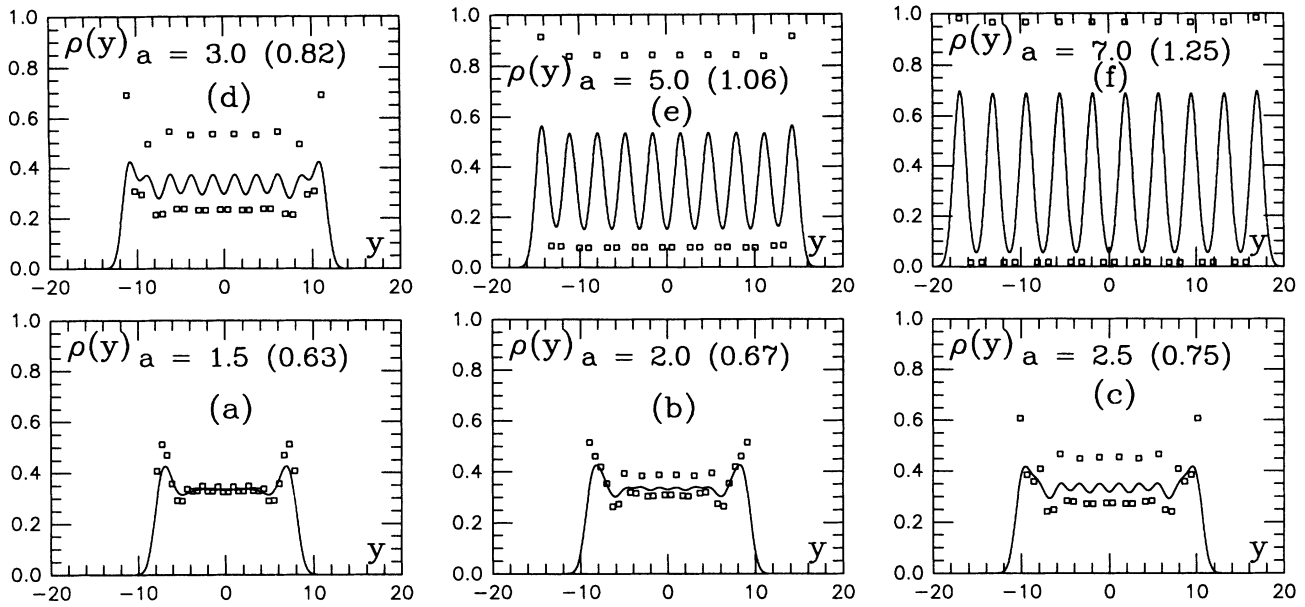


FIG. 2. Same as Fig. 1, except γ is increased further, stretching the cylinder. The charge-density wave state starts to appear at an aspect ratio of 2 and is fully developed at 5.

squeezed direction (see Fig. 3). We have found several interesting properties of the Laughlin's wave function for $\gamma=0$ which we now address. In this limit, Ψ_L assumes the familiar form:

$$\Psi_L^{\gamma=0} = \prod_{i < j} (z_i - z_j)^m \prod_i e^{-y_i^2/2l^2}. \quad (5)$$

Clearly in the expansion of this wave function all occupation amplitudes are integers. In particular, expanding the Jastrow factor we obtain

$$\prod_{i < j} (z_i - z_j)^m = \sum_{m_1, m_2, \dots, m_N} C(m_1, m_2, \dots, m_N) \prod_{i=1}^N z_i^{m_i}. \quad (6)$$

In the Appendix, we show that

- (a) $C(\{m_{p_i}\}) = (-1)^P C(\{m_i\})$, P is a permutation on N objects.
- (b) $C(\{m_i^0\}) = 1$, where $\{m_i^0\} = \{m(i-1)\}$.
- (c) $C(\{m_i\}) = m \times \text{integer}$, (integer can be zero) if $\{m_i\}$ can be obtained from a permutation of $\{m_i^0\}$ by a succession of "squeezing" operations (defined below).

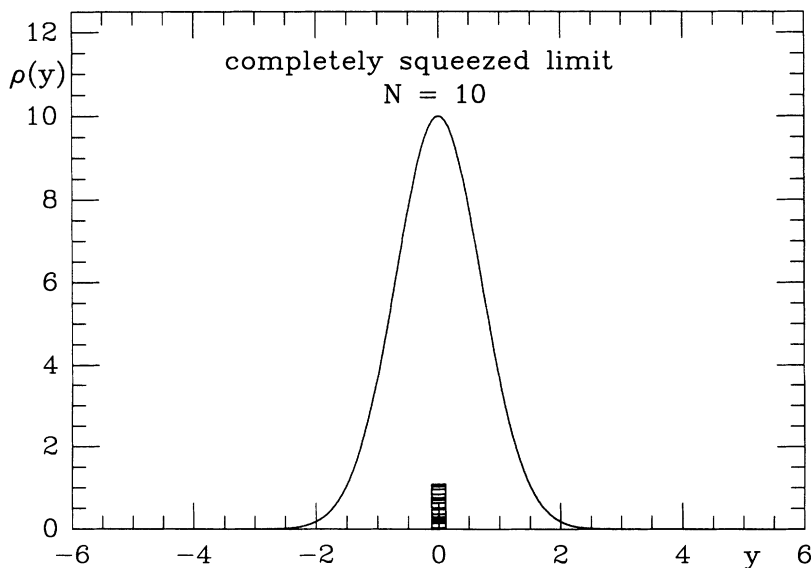


FIG. 3. The charge density of the completely squeezed cylinder. The occupation amplitudes are now centered at $y=0$ since no motion of the Gaussian envelope is possible in the squeezed direction. The units of the density in this figure are arbitrary and independent of those in Figs. 1 and 2. $N=10$ in this case as well.

(d) $C(\{m_i\})=0$ if $\{m_i\}$ is not a permutation of $\{m_i^0\}$ or a configuration obtained by successive “squeezing” of $\{m_i^0\}$.

The squeezing operation (without reordering) $\{m_i\} \rightarrow \{m'_i\}$ is defined for some pair $j \neq k$ with $m_j > m_k$ and a positive integer n by

$$\begin{aligned} m'_i &= m_i \quad \text{if } i \neq j, k \\ m'_j &= m_j - n, \\ m'_k &= m_k + n, \end{aligned}$$

where $0 < n < m_j - m_k$.

Note that

$$\begin{aligned} \sum_{i < j} (m_i - m_j)^2 &> \sum_{i < j} (m'_i - m'_j)^2 \\ &= \sum_{i < j} (m_i - m_j)^2 + 2nN[n - (m_j - m_k)]. \end{aligned}$$

Since every occupation state with nonzero amplitude can be squeezed from the TT state and, since within constants, $\sum_i n_i^2$ is related to $\sum_{i < j} (n_i - n_j)^2$, it can be seen from Eq. (4) that the above inequality implies that the TT state will dominate the wave function as $\gamma \rightarrow \infty$. In practice, this condition is realized for $\gamma \geq 1$, see Fig. 2.

We have also empirically verified the following for up to $N=8$ electron systems, the proof of which we leave as an open problem:

- (1) The filled level droplet has the highest amplitude.
- (2) $A(\text{filled level droplet}) = ((-1)^{[(N+2)/(m-1)]} \{[(m+1)/2]N\}!) / \{N![(m+1)/2]!^N\}$.
- (3) The total normalization is $\|\Psi\|^2 = |mN|! / (N!|m|!^N)$.

The first four items (a)–(d) are also valid for bosons except of course the wave function is now symmetric. The last three items (1)–(3) are however only valid for fermions.

It should be noted here that in the squeezed limit, the appropriate 1D Hamiltonian for which the $\nu = \frac{1}{3}$ Laughlin state is an exact zero-energy ground state is

$$H(x_1, x_2, \dots, x_N) = - \sum_{i < j} \frac{\partial^2}{\partial x_i^2} \delta(x_i - x_j). \quad (7)$$

This result also noticed by Wen is an obvious limit of the full two-dimensional hard-core potential.^{2,9}

Before we study edge states, we would like to make a few comments. The period of the oscillation of the density near the edges in the fluid phase is determined by the bulk density-density response function which is dominated by a single mode, namely, the magnetoroton.¹⁰ As such, it is similar to the impurity screening (or the lack of it) by the incompressible fluid. The period at the edge is comparable to that of the density oscillations near an impurity.¹¹ In the limit of large aspect ratios, the system makes a transition to a “stripped Wigner Crystal” phase where the number of peaks in the density is equal to number of electrons. This same limit, but for the Coulomb interactions, has been studied by Chui¹² in connection with narrow channels. However, he used toroidal boundary conditions. It is not surprising to see gapless modes¹³ (as we see) in this limit. In the opposite limit, e.g., small γ , the gap survives at least for the hard-core repulsion and may be the more appropriate limit for narrow channel geometries. Whether or not QHE can be ruled out for very narrow channels has not yet been addressed in our study and needs further investigation.

We next turn to the discussion of edge excitations of the Laughlin droplet (or ribbon in our case). Again, the most interesting limit turns out to be the completely squeezed cylinder ($\gamma=0$). In this limit, there is no bulk in the usual sense and only edge excitations remain. Wen¹⁴ has used current algebra techniques to study edge states with the same results as here. One of us¹⁵ has interpreted the edge states as “generalized Fermi-surface singularities,” obeying a generalized Luttinger¹⁶ theorem. Here we follow that formalism.

Consider first a free Fermi gas with a momentum space energy surface $E(k)$ having the topology shown in Fig. 4. In terms of the Fermi points k_f^i , we have the Luttinger theorem for the total number of particles N and the total momentum of the system P :

$$N = \frac{L}{2\pi} \sum_i \Delta v_i k_f^i, \quad (8)$$

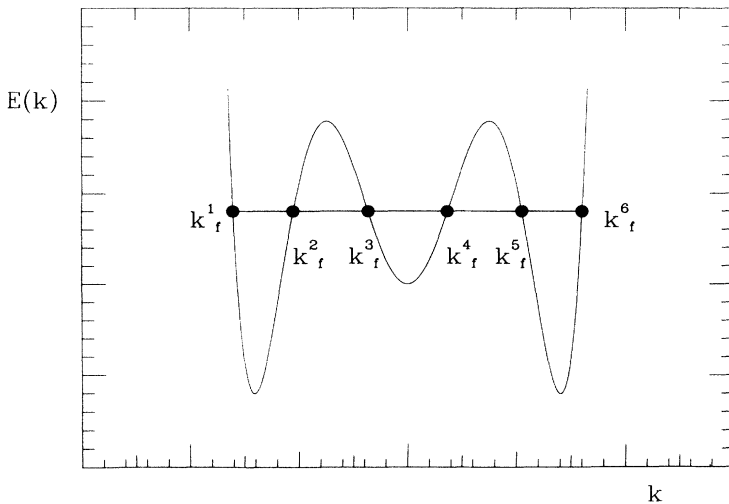


FIG. 4. An arbitrary energy versus momentum dispersion relation $E(k)$ for a 1D Fermi gas. The Fermi energy is shown by the horizontal line and the Fermi points are labeled.

$$P = \frac{L}{4\pi} \sum_i \Delta v_i (k_f^i)^2, \quad (9)$$

where $\Delta v = n(k_f - \epsilon) - n(k_f + \epsilon)$ is the jump across the Fermi point, and L is the length of the system. One can generalize these expressions to contain local deviations of the Fermi points $\delta k_f^i(x)$ from their uniform value k_f^i :

$$\Delta \rho(x) = \frac{1}{2\pi} \sum_i \Delta v_i \delta k_f^i(x), \quad (10)$$

$$\Delta \Pi(x) = \frac{1}{2\pi} \sum_i \Delta v_i k_f^i \delta k_f^i(x) + \frac{1}{4\pi} \sum_i \Delta v_i (\delta k_f^i(x))^2, \quad (11)$$

where

$$k_f^i(x) = k_f^i + \frac{2\pi \rho_i(x)}{\Delta v_i}, \quad (12)$$

$$\rho(x) = \frac{N}{L}, \quad (13)$$

$$\Pi(x) = \frac{P}{L}. \quad (14)$$

The local description is valid only if for any pair of indices i, j the condition $(k_f^i - k_f^j)\xi \gg 1$ is satisfied. Here, ξ is an inverse momentum cutoff measured from the Fermi points.

Similarly the Hamiltonian for edge deformation can be expressed in terms of the local fluctuations of the Fermi wave vector:

$$H^{(0)} = \frac{1}{4\pi} \int dx \sum_i v_f^i \Delta v_i (\delta k_f^i(x))^2, \quad (15)$$

where v_f^i 's are the Fermi velocities. It is possible to include interactions terms between these fluctuations as in Fermi-liquid theory but such terms are not relevant to this work and will not be pursued here. We next proceed to quantization.

It is well known that for 1D Fermi gas,¹⁷ the Fourier components of the density operators (Tomonaga bosons)

$$\rho_q^i(x) = \frac{1}{L} \sum_{|q| < \xi^{-1}} e^{iqx} \rho_q^i, \quad (16)$$

satisfy the Kac-Moody algebra:

$$[\rho_q^i, \rho_{q'}^j] = \Delta v_i \delta_{i,j} \frac{qL}{2\pi} \delta_{q+q',0}, \quad q\xi \ll 1. \quad (17)$$

Furthermore, Bosonizations of Fermi fields in 1D give

$$\Psi_i^\dagger(x) = A_i e^{i \int_{-\infty}^x dx' k_f^i(x')} \quad (18)$$

$$= A_i e^{i\phi_i(x)}, \quad (19)$$

where A_i , to be given shortly, are operators which make Ψ 's anticommute, and $\phi_i(x)$ is the canonical Bose field. From these and Eq. (12), we obtain

$$\frac{\partial \phi_i}{\partial x} = k_f^i(x) \quad (20)$$

$$= k_f^i + \frac{2\pi \rho_i(x)}{\Delta v_i}, \quad (21)$$

which is the ‘‘chiral constraint.’’ Next, from the above equations, we obtain the commutation rules (CR):

$$[\rho_i(x), \rho_j(x')] = \delta_{i,j} \frac{\Delta v_i}{2\pi} \frac{d}{dx} [\delta(x-x')], \quad (22)$$

$$\left[\rho_i(x), \frac{\partial \phi(x')}{\partial x'} \right] = \delta_{i,j} \frac{d}{dx} [\delta(x-x')], \quad (23)$$

$$[\phi_i(x), \rho_j(x')] = i \delta_{i,j} \delta(x-x'), \quad (24)$$

$$\left[\phi_i(x), \frac{\partial \phi(x')}{\partial x'} \right] = 2\pi i \Delta v_i \delta_{i,j} \delta(x-x'), \quad (25)$$

$$[\phi_i(x), \phi_j(x')] = \frac{i\pi}{\Delta v_i} \delta_{i,j} \text{sgn}(x-x'), \quad (26)$$

where sgn denotes the sign function. Thus ϕ and ρ (or the derivative of ϕ) are conjugate fields. Using these CR's and

$$[N, \Psi_i^\dagger(x)] = \Psi_i^\dagger(x), \quad (27)$$

it can be seen that

$$\Psi_i^\dagger(x) \Psi_i(x') = \Psi_i(x') \Psi_i^\dagger(x) e^{-[\phi_i(x), \phi_i(x')]} \quad (28)$$

For the fields to obey Fermi statistics, we must require that $1/\Delta v$ be an odd integer $\pm m$. We also note that the choice

$$A_i = e^{i\pi/2 \sum_j \text{sgn}(i-j) N_j} \quad (29)$$

makes the Fermi fields for different sectors ($i \neq j$) anticommute as well.

The usual results for the 1D Fermi gas are recovered when $\Delta v = 1$. On the other hand, applying this formalism to the quantum Hall effect, we obtain $\Delta v = 1/m$. The CR's for the Bose fields $\phi(x)$ in these two cases are therefore related by

$$[\phi(x), \phi(x')]_{\text{QHE}} = \frac{1}{m} [\phi(x), \phi(x')]_{\text{Fermi}}. \quad (30)$$

Following standard treatment of the Luttinger model,¹⁷ except here one needs to consider only a single branch of fermions (for example the right moving one), the single-particle Green's function is

$$G(x-x', t-t') = \left[\frac{1}{x-x'-v_f(t-t')} \right]^m e^{imk_f(x-x')}. \quad (31)$$

Fourier transforming the equal time Green's function, we obtain the average occupation:

$$n(k) \approx C \frac{(k - mk_f)^m}{|k - mk_f|} + n^{\text{reg}}(k), \quad (32)$$

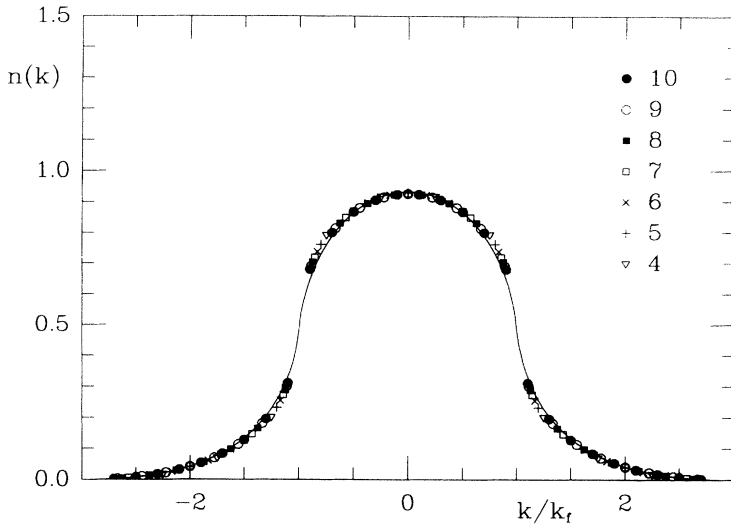


FIG. 5. The average occupation of $n(k)$ versus k for the Laughlin state at $\frac{1}{3}$ filling for up to ten electron-size systems. The k axis has been normalized by k_f so that $k/k_f = 2m_i/N$, $m_i = -m(N-1)/2, \dots, m(N-1)/2$. The solid curve is the exact $n(k)$ for the Calogero-Sutherland model.

where C is a numerical coefficient and $n^{\text{reg}}(k)$ is the non-singular part of $n(k)$. The average occupation of the edge excitations must therefore exhibit a power-law singularity at mk_f with exponent $m-1$. We next present numerical results. From here on we will only consider the completely squeezed geometry $\gamma=0$.

Figure 5 shows $n(k)$ for up to ten electron-size systems for $\nu = \frac{1}{3}$. As can be seen, there is a remarkable degree of convergence and the shape of $n(k)$ is already clear. We have defined $k_f(N)$ for each size by having exactly N states between $-k_f \leq k \leq k_f$. For each size, we have rescaled k in Fig. 5 by k_f . The solid curve is $n(k)$ of the Calogero-Sutherland¹⁸ model. It was obtained from a conjecture by Haldane¹⁹ giving the full analytical expression of the retarded Green's function for the Calogero-Sutherland model at integer coupling ($\lambda=m$ for $\nu=1/m$). Haldane's expression reduces to the equal time Green's function recently calculated by Forrester.²⁰ Note that in Fig. 5, there appears to be a weakly singular pseudo-Fermi surface at k_f . The singularity of interest,

however, is not at k_f but at mk_f , i.e., $3k_f$ in this case. Unfortunately, even $N=10$ is not sufficiently large to make a direct extrapolation of the exponent possible (see below, however). That is, we have not approached the $k=3k_f$ sufficiently closely (see Fig. 5). However, we extract the exponent as follows: we observe that the last possible k for which $n(k)$ is nonzero satisfies $(k_{\text{max}} - 3k_f) \sim 1/N$ (see caption to Fig. 5). Now if $n(k) \sim (k - 3k_f)^2$ then $n(k_{\text{max}}) \sim 1/N^2$, which implies that, in the thermodynamic limit the quantity $N^2 n(k_{\text{max}})$ should extrapolate to a finite value. Figure 6 shows such an extrapolation clearly demonstrating the $(k - 3k_f)^2$ dependence. The value of this exponent has also been confirmed in the planar disk geometry.²¹

At first sight, the data in Fig. 5 seems to be size independent and to exactly form a universal curve. This is not so, there are extremely small finite-size effects. In fact, we have empirically obtained the exact expression for the last 4 of $n(k)$ in the tail of the distribution as a function of system size:

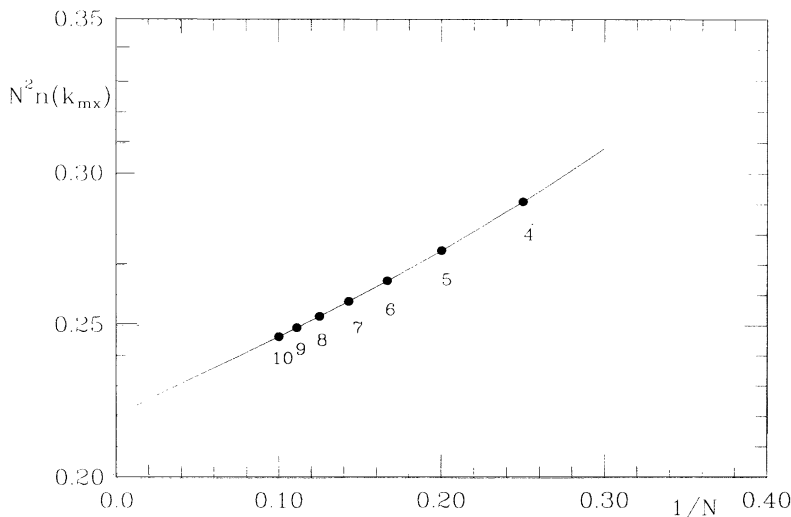


FIG. 6. The plot of $N^2 n(k_{\text{max}})$ versus $1/N$. An estimate of $N^2 n(k_{\text{max}})$ as $N \rightarrow \infty$, based on the extrapolation of the data, yields 0.22.

$$n_0 = \frac{2}{2+9N(N-1)},$$

$$n_{-1} = \frac{18(N-1)}{[2+9N(N-1)][1+3(N-2)]},$$

$$n_{-2} = \frac{36(N-1)(9N^2-30N+22)}{[2+9N(N-1)][2+9(N-1)(N-2)][1+3(N-3)]},$$

$$n_{-3} = \frac{4[2+3(N-3)](405N^4-2970N^3+7425N^2-7554N+2698)}{[2+9N(N-1)][2+9(N-1)(N-2)][2+9(N-2)(N-3)][1+3(N-4)]},$$

where $n_0 \equiv n(k_{\max})$, $n_{-1} \equiv n(k_{\max-1})$, etc. One might wonder if there is a pattern to be used for constructing successively higher terms. While the factors in the denominator appear to follow a simple pattern, it is clear that the one polynomial in the numerator rapidly becomes complicated and is not easily generalized. However, it should be noted that, as $N \rightarrow \infty$, the ratio of these coefficients become very simple:

$$\frac{n_0}{n_0} = 1, \quad (33)$$

$$\frac{n_{-1}}{n_0} = 3, \quad (34)$$

$$\frac{n_{-2}}{n_0} = 6, \quad (35)$$

$$\frac{n_{-3}}{n_0} = 10. \quad (36)$$

This sequence makes it clear that these ratios are just the expansion coefficient of $(1-x)^{-3}$. That is,

$$\frac{n_{-p}}{n_0} = \frac{(p+1)(p+2)}{2}.$$

This particular increasing sequence has also been noticed by Wen.²² We note in passing that the simple extrapolation procedure in Fig. 6, where we essentially extend the line connecting the points $N=10$ and 9, out to $N=\infty$,

gives the value of 0.22 for the coefficient of N^{-2} , which is remarkably close to the exact $\frac{2}{9}$ answer. It should also be noted here that one can directly extract the exponent from the analytical expression of n_0 by using the identity

$$\frac{k - mk_f}{k_f} = -\frac{m}{N} \quad (m=3)$$

to eliminate N in favor of $k - 3k_f$.

We have also calculated the average occupations for the boson Laughlin state at $\nu = \frac{1}{2}$. Here, the exact analytical form of $n(k)$ is known²³

$$n(k) = C' \Theta(2k_f - k) \ln \frac{2k_f}{k}, \quad (37)$$

where C' is another constant and Θ is the step function. Note that the logarithmic dependence upon k predicts a linear relation between $n(k)$ and $k - 2k_f$, which is clearly seen in Fig. 7. It should also be noted that the increase of $n(k)$ with size at $k=0$ is highly suggestive of a weak singularity, consistent with the logarithmic form in Eq. (33). This singularity is however an artifact of the squeezed limit and will disappear for nonzero γ as will the singularity at k_f in the Fermi case.

There are, in the realm of the quantum Hall effect, other states with perhaps more interesting edge excitations. We will not address all such states here but confine our attention to the pairing ones which have been proposed as candidates for the $\nu = \frac{5}{2}$ Hall state. First, a spin-singlet

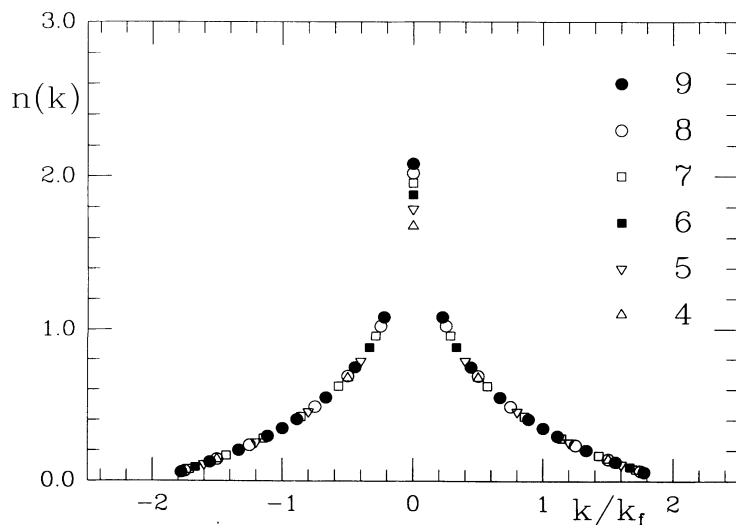


FIG. 7. Same as Fig. 5, but for bosons at $\nu = \frac{1}{2}$. Here there is a hint of the logarithmic singularity in the exact result for $N \rightarrow \infty$ (see text) at $k=0$. The logarithmic dependence yields a linear exponent at $2k_f$ which can be seen in this plot.

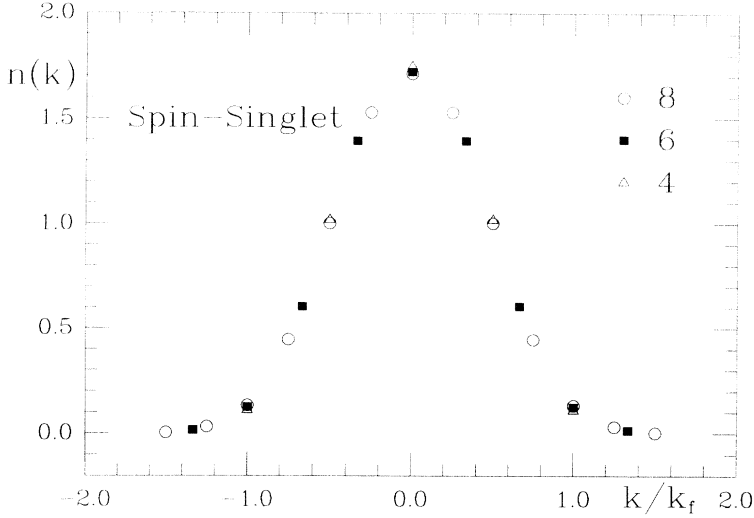


FIG. 8. Same as Fig. 5, except for the spin-singlet pairing state of Eq. (38). $n(k)$ is similar to the single-particle occupation in the BCS ground state with no singularity at k_f .

state was proposed by us:²⁴

$$\Psi_{\text{HR}} = \prod_{i < j} (z_i^\uparrow - z_j^\uparrow)^2 \times \prod_{i < j} (z_i^\downarrow - z_j^\downarrow)^2 \times \prod_{i,j} (z_i^\uparrow - z_j^\downarrow)^2 \text{Det} \left\{ \frac{1}{(z_i^\uparrow - z_j^\downarrow)^2} \right\}, \quad (38)$$

where Det stands for the determinant.

The other a spin-polarized state was proposed by Moore and Read²⁵ and later studied by Greiter, Wen, and Wilczek.²⁶

$$\Psi_{\text{MR}} = \prod_{i < j} (z_i - z_j)^2 \text{Pf} \left\{ \frac{1}{(z_i - z_j)} \right\}, \quad (39)$$

where Pf denotes the Pfaffian. Both the determinant and the Pfaffian act to create pairs and are closely related to BCS wave function for singlet and triplet pairing respec-

tively. One, therefore, might expect as in BCS theory a smoothly falling $n(k)$ with no semblance of any singularity at k_f that was seen for the $\frac{1}{3}$ state. This is clearly borne out in Fig. 8 showing $n(k)$ for the spin-singlet state for up to eight electrons. There is indeed a marked difference from that of the Laughlin wave function. There is evidently, as before, a reasonable degree of convergence already with these small sizes.

Analogous results for the spin-polarized Pfaffian state^{25,26} is shown in Fig. 9. There is a rather sharp drop at k_f possibly indicating a weak singularity, i.e., a pseudo-Fermi surface, which is probably an artifact of the squeezed limit. In addition, it shows a very slight dip at $k=0$. Despite their common pairing nature, the two $n(k)$ of Figs. 8 and 9 appear to be different. Presumably because of the differences in even (spin-singlet) or odd pairing states of the two. A more detailed understanding of these differences will probably have to await until a more precise analytical expression for $n(k)$ is obtained.

In closing we emphasize again that while for convenience we have studied the edge states in the squeezed limit

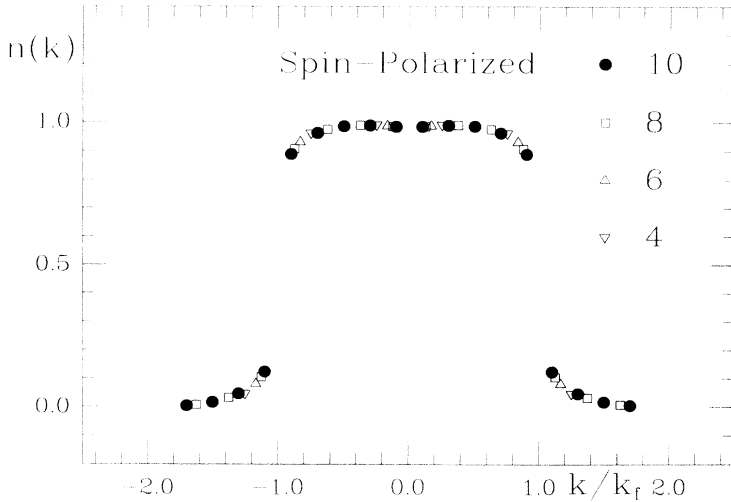


FIG. 9. Same as Fig. 8, but for the Pfaffian pairing state.

$\gamma=0$, our results on the edge singularity remain valid for all aspect ratios $\gamma \neq 0$ so long as the bulk is an incompressible fluid. As stated earlier only the apparent singularities at $k=k_f$ for fermions and $k=0$ for bosons are washed out at nonzero γ .

This work was supported by NSF Grants DMR-9113876 at CSULA, and DMR-922407 at Princeton University.

APPENDIX

The first property follows from the antisymmetry of the wave function. We find the state with the smallest amplitude by choosing the configuration with lowest power of z_1 , then lowest power of z_2 , etc. We obtain

$$(-)^N \prod_{j=2}^n z_j^m \prod_{j=3}^N z_j^m \cdots z_N^{m(N-1)} = (-)^N \sum_{j=2}^N z_j^{m(j-1)}. \quad (\text{A1})$$

From this we immediately pick out the occupation numbers:

$$n_j = \begin{cases} 1 & \text{for } j=0, m, 2m, \dots, Nm, \\ 0 & \text{otherwise} \end{cases} \quad (\text{A2})$$

$$(\text{A3})$$

Thus, every m th orbital is occupied, which is the TT state. Note that TT state in configuration space can be obtained by antisymmetrization of this expression (see

below). There is another more direct way of seeing this which also will prove point c . We expand the polynomial in the following manner:

$$\prod_{i < j} (z_i - z_j)^m = \prod_{i < j} (z_i^m - z_j^m + mX_{i,j}) \quad (\text{A4})$$

$$\times \prod_{i < j} (z_i^m - z_j^m) + m \prod_{i < j} G_{i,j}. \quad (\text{A5})$$

The first term is the TT state with a coefficient of unity. $X_{i,j}$ and $G_{i,j}$ are appropriate remainder terms. It can be seen from the binomial expansion that a factor of m multiplies $X_{i,j}$ and hence $\prod_{i < j} G_{i,j}$. This proves point c .

To establish the ‘‘squeezability’’ we write

$$\prod_{i < j} (z_i - z_j)^m = \prod_j z_j^{m(N-j)} \prod_{i < j} \left[1 - \frac{z_j}{z_i} \right]^m. \quad (\text{A6})$$

Note the prefactor is related to a similar expression given above Eq. (7) by the permutation

$$\begin{bmatrix} 1 & 2 & \cdots & N \\ N & N-1 & \cdots & 1 \end{bmatrix},$$

with the correct sign $(-)^N$, and thus it describes the TT state. Now consider any pair k, l with $k > l$, since in the prefactor z_l is raised to a higher power than z_k , but in the product $\prod_{i < j} (1 - z_i/z_j)$, j is greater than i , it then follows that the power of z_l will increase while the power of z_k will decrease, indicating the pair is being squeezed together.

¹R. B. Laughlin, Phys. Rev. Lett. **50**, 1395 (1983).

²F. D. M. Haldane, in *The Quantum Hall Effect*, edited by R. E. Prange and S. M. Girvin, Graduate Texts in Contemporary Physics (Springer-Verlag, New York, 1986).

³F. D. M. Haldane, Phys. Rev. Lett. **51**, 645 (1983); F. D. M. Haldane and E. H. Rezayi, *ibid.* **54**, 237 (1985).

⁴F. D. M. Haldane, Phys. Rev. Lett. **55**, 2095 (1985).

⁵D. J. Yoshioka, B. I. Halperin, and P. A. Lee, Phys. Rev. Lett. **50**, 1219 (1983).

⁶D. J. Thouless, Surf. Sci. **142**, 147 (1984).

⁷R. Tao and D. J. Thouless, Phys. Rev. B **28**, 1142 (1983).

⁸Kenichi Takano and A. Ishihara, Phys. Rev. B **34**, 1399 (1986).

⁹S. Trugman and S. Kivelson, Phys. Rev. B **31**, 5280 (1985).

¹⁰S. M. Girvin, A. H. MacDonald, and P. M. Platzman, Phys. Rev. Lett. **54**, 581 (1985).

¹¹F. C. Zhang, V. Z. Volovic, Y. Guo, and S. Das Sarma, Phys. Rev. B **32**, 6920 (1985); E. H. Rezayi and F. D. M. Haldane, *ibid.* **32**, 6924 (1985).

¹²S. T. Chui, Phys. Rev. Lett. **56**, 2395 (1986).

¹³As one would expect from a Wigner-Crystal-like ground state.

¹⁴X. G. Wen, Phys. Rev. Lett. **64**, 2206 (1990); Phys. Rev. B **41**, 12 838 (1990).

¹⁵F. D. M. Haldane, in *Perspectives in Many-Particle Physics*

(Proceedings of the International School of Physics ‘‘Enrico Fermi,’’ Varenna on Lake Como, 1992, edited by R. A. Broglia and J. R. Schrieffer (North-Holland, Amsterdam, 1994), pp. 5–29.

¹⁶J. M. Luttinger, Phys. Rev. **119**, 1153 (1960).

¹⁷For review and additional references, see J. Solyom, Adv. Phys. **28**, 201 (1979).

¹⁸F. Calogero, J. Math. Phys. **10**, 2191 (1969); B. Sutherland, *ibid.* **12**, 246 (1971); Phys. Rev. Lett. **54**, 581 (1985).

¹⁹F. D. M. Haldane, in *Proceedings of the 16th Taniguchi Symposium, Kashikojima, Japan, October 26–29, 1993*, edited by A. Okiji and N. Kawakami (Springer, Berlin, 1994).

²⁰P. J. Forrester, Phys. Lett. A **179**, 127 (1993).

²¹S. Mitra and A. H. MacDonald, Phys. Rev. B **48**, 2005 (1993).

²²X. G. Wen (private communication).

²³F. J. Dyson, J. Math. Phys. **3**, 140 (1962); Phys. Rev. Lett. **54**, 581 (1985).

²⁴F. D. Haldane and E. H. Rezayi, Phys. Rev. Lett. **60**, 956 (1988); **60**, 1886(E) (1988).

²⁵G. Moore and N. Read, Nucl. Phys. B **360**, 362 (1991).

²⁶M. Greiter, X.-G. Wen, and F. Wilczek, Phys. Rev. Lett. **66**, 3205 (1991).